

# HEAT TRANSFER STUDY FROM SQUARE CYLINDER IMMERSED IN WATER-BASED NANOFLUID: EFFECT OF ORIENTATION

Jaspinder Kaur, Jatinder Kumar Ratan, Anurag Kumar Tiwari\*

Dr B.R. Ambedkar National Institute of Technology Jalandar Punjab,  
Chemical Engineering Department, Pin code 144011, India

Heat transfer study from the heated square cylinder at a different orientation angle to the stream of nanofluids has been investigated numerically. CuO-based nanofluids were used to elucidate the significant effect of parameters: Reynolds number (1–40), nanoparticle volume fraction (0.00–0.05), the diameter of the *NPs* (30–100 nm) and the orientation of square cylinder (0–90°). The numerical results were expressed in terms of isotherm contours and average Nusselt number to explain the effect of relevant parameters. Over the range of conditions, the separation of the boundary layers of nanofluids increased with the size of the *NPs* as compared to pure water. *NPs* volume fraction and its size had a significant effect on heat transfer rate. The square cylinder of orientation angle (45°) gained a more efficient heat transfer cylinder than other orientation angles. Finally, the correlations were developed for the average Nusselt number in terms of the relevant parameters for 45° orientation of the cylinder for new applications.

**Keywords:** inclined square cylinder, nanofluids, Reynolds number, Prandtl number, steady flow regime

## 1. INTRODUCTION

*Nanofluids* have gained a lot of attention from researchers due to many applications in various fields such as energy, bio, and pharmaceutical industry and chemical, environmental, materials, medical and thermal engineering. Nanofluids have gained significant attention due to their enhanced thermal characteristics as compared to base fluids. Over the last few decades, the heat transfer from a bluff body of different shapes to nanofluids has been frequently used in many industrial applications, for instance, pin-type and tubular heat exchangers, cooling of nuclear fuel rods and various electronic components, etc. Among various configurations of the bluff body, the circular cylinder has been studied more extensively due to its frequent occurrence in many practical applications which is found in Chhabra and Richardson (2011). In contrast to the circular cylinder, not only knowledge of the square cross-section of the cylinder is very limited, but also there is additional complexity arising from an orientation of the cylinder with respect to the incoming

\* Corresponding author, e-mail: [tiwaria@nitj.ac.in](mailto:tiwaria@nitj.ac.in)

<https://journals.pan.pl/cpe>

Presented at the International Chemical Engineering Conference 2021 (ICHEEC): 100 Glorious Years of Chemical Engineering and Technology, held from September 16–19, 2021 at Dr B. R. Ambedkar National Institute of Technology, Jalandhar, Punjab, India.



nanofluids. All the reported results related to heat transfer indicated the varying levels of augmentation in heat transfer under appropriate conditions. For instance, Valipour and Ghadi (2011) have numerically investigated the flow and heat transfer over a circular cylinder for copper-based aqueous nanofluids in the range of  $Re \leq 40$  and  $\phi \leq 0.05$ . In the results part, the Nusselt number is seen to increase with the volume fraction of the nanoparticles. Furthermore, a similar study has been done by Etminan-Farooji et al. (2012) in the case of a square cylinder ( $0^\circ$  inclined) in nanofluids with two types of nanofluids comprised of  $Al_2O_3$  and CuO nanoparticles. Depending upon the type of nanofluids, an enhancement in heat transfer up to 25% in comparison with pure water can be seen at higher values of the Peclet number and particle volume fraction. From the literature, it is clear that there is no investigation available on the heat transfer phenomena from a square cylinder at different orientation angles in the uniform flow of nanofluids. This particular shape of the cylinder is important for many process industries (such as novel heat exchangers, various electronic components). Therefore it is important to investigate numerical study of heat transfer from the two-dimensional flow of water base nanofluids over a square cylinder carried out in the laminar steady flow regime. The present numerical results are expressed in terms of isotherm contours (temp, average Nusselt number and discussed the effect of Reynolds number ( $1 \leq Re \leq 40$ ), nanoparticle volume fraction ( $0 \leq \phi \leq 0.05$ ), nanoparticles (CuO), and particle size  $d_{np}$  at constant wall thermal boundary condition (CWT). In the end, the present numerical results have developed the correlation for average Nusselt number for further application.

## 2. PROBLEM STATEMENT

The two-dimensional flow over a square cylinder (size  $a$ ) to the oncoming uniform stream of nanofluids with velocity  $V_\infty$  and at temperature,  $T_\infty$  is shown schematically in Fig. 1. The surface of the square cylinder is maintained at a constant wall temperature  $T_w$  (CWT) boundary. To make this unconfined flow problem numerically feasible, an artificial cylindrical domain of nanofluids of diameter  $D_\infty$  is considered in which the square cylinder is placed at the centre of the domain (see Fig. 1b). Over the range of parameters, the flow is assumed to be steady, incompressible, and the laminar flow domain is carried out to minimize the computational efforts. The thermo-physical properties of nanofluids such as density,  $\rho_{nf}$ , (Pak and Cho, 1998), specific heat,  $C_{p,nf}$ , (Xuan and Roetzel, 2000), thermal conductivity,  $k_{nf}$ , (Koo and Kleinstreuer, 2004) and viscosity,  $\mu_{nf}$ , (Masoumi et al., 2009) are calculated as a function of nanoparticle volume fraction,  $\phi$ , together with properties of the base fluid and NPs.

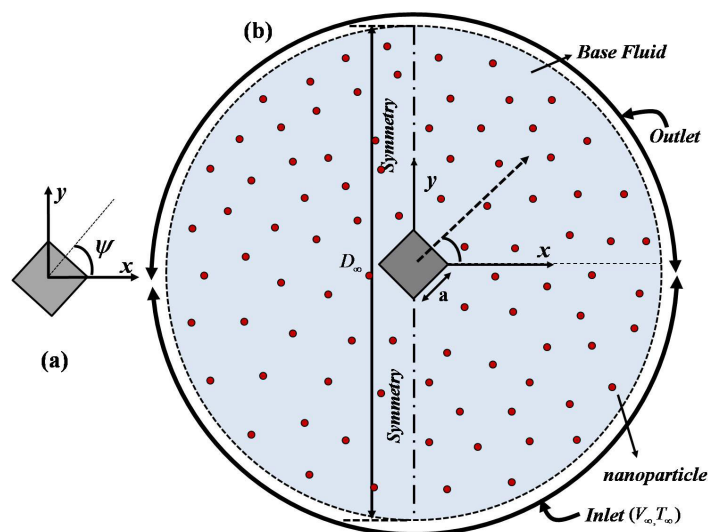


Fig. 1. Schematic representation of the problem of flow past and heat transfer from (a) square cylinder, (b) computational domain

Since the thermo-physical properties of the nanofluids are assumed to be temperature-dependent; the velocity and temperature fields are coupled in nature. The viscous dissipation effects are neglected. Within the framework of the above assumptions, the coupled velocity and temperature fields are described by the following mass, momentum, and energy:

- continuity equation:

$$\Delta V = 0 \quad (1)$$

- momentum equation:

$$\rho_{nf} (V \nabla) V = -\nabla p + \nabla \cdot (\mu_{nf} \nabla V) \quad (2)$$

- thermal energy equation:

$$\rho_{nf} C_{nf} (V \nabla) T = \nabla \cdot (k_{nf} \nabla T) \quad (3)$$

The specified boundary conditions are used lower-half of the domain as an inlet condition (i.e.,  $V_x = 1$ ,  $V_y = 0$ ,  $T = 300^\circ$ ), no-slip and constant wall temperature on the surface of the square cylinder is defined condition (i.e.,  $V_x = V_y = 0$ ,  $T = 305^\circ$ ), and upper-half of the artificial cylindrical (i.e.,  $\frac{\partial \varphi}{\partial x} = 0$ , where  $V_x$ ,  $V_y$  and  $T$ ).

Finally, the governing equations subjected to the above boundary conditions are solved in terms of the primitive variables ( $V_x$ ,  $V_y$ ,  $p$ ,  $T$ ) and results are post-processed to evaluate the average value of Nusselt number.

$$\text{Nu}_{\text{avg}} = \frac{1}{S} \int_0^S \text{Nu} \, ds \quad (4)$$

The extensive numerical results in the present study are expressed in terms of drag coefficient and Nusselt numbers are expected to be a function of  $\text{Re}$ ,  $\phi$ ,  $d_{np}$  and this work endeavours to explore this functional relationship for nanofluids past a heated square cylinder at different orientations.

### 2.1. Numerical solution procedure and computational parameters

The finite element method-based commercial software COMSOL Multiphysics® was used to solve the governing differential equations along with boundary conditions. Detailed numerical descriptions of the solution methodology are available in the literature [Kaur et al. \(2021\)](#). A simulation was deemed to have converged when the relative residuals for the momentum equations were lower than  $10^{-7}$ . This was also sufficient to ensure that the drag values stabilized at least up to four significant digits. The Lagrangian scheme was used to solve the pressure-velocity coupling. The optimum size of the domain,  $D_\infty/a = 150$  is adequate for this present computational study. The minimum number of a grid with the total number of elements,  $N = 56298$  was found to be sufficient for the present study over the wide range of conditions considered herein.

## 3. RESULTS AND DISCUSSION

### 3.1. Validation of results

To check the accuracy and confidence of the present numerical results, it is important to validate the current numerical methodology. The validation result for forced convection heat transfer phenomena from a square cylinder immersed in water base nanofluids (CuO) is represented in Table 1. The average heat transfer coefficient is calculated for the square cylinder in the infinite extent of nanofluids and compared with [Etminan-Farooji et al. \(2012\)](#). The results are seen to be in good agreement, thus, the present numerical results are believed to be reliable to within 3–4%.

Table 1. Validation of average heat transfer coefficient for a square cylinder in Al<sub>2</sub>O<sub>3</sub>/water and CuO/water nanofluids ( $\phi = 0.04$ )

Pe = Re · Pr	$d_{np} = 30 \text{ nm}$		$d_{np} = 100 \text{ nm}$	
Al <sub>2</sub> O <sub>3</sub>	Present	Etminan-Farooji et al. (2012)	Present	Etminan-Farooji et al. (2012)
50	2.0131	2.1404	2.1162	2.2275
100	2.6931	2.8714	2.9847	3.0067
200	3.7497	3.9593	3.9795	4.1337
Pe = Re · Pr	$d_{np} = 30 \text{ nm}$		$d_{np} = 100 \text{ nm}$	
CuO	Present	Etminan-Farooji et al. (2012)	Present	Etminan-Farooji et al. (2012)
50	2.1310	2.2728	2.1086	2.2728
100	3.0103	3.0610	3.0095	3.0591
200	4.0899	4.1660	4.0288	4.1660

### 3.2. Isotherm contours

Fig. 2 represents the isotherm contours near the square cylinder at  $Re = 10$  and  $Re = 40$  for two different sizes of NPs,  $d_{np} = 30 \text{ nm}$  and  $d_{np} = 100 \text{ nm}$  for three different orientation angles  $\psi = 0, 45^\circ$  and  $75^\circ$ . At a low value of  $Re$  ( $Re < 10$ ), the isotherm contours are less crowded near the heated cylinder and weak temperature gradients in the flow domain. Because of the increased amount of inertia force, the crowding of the isotherm contours towards the surface of the cylinder occurs when the Reynolds number ( $Re > 10$ ) increases. This crowding of isotherm contours is seen to be more pronounced on the downstream side of the cylinder due to the large wake formation. The isotherm contours are also crowded with orientation

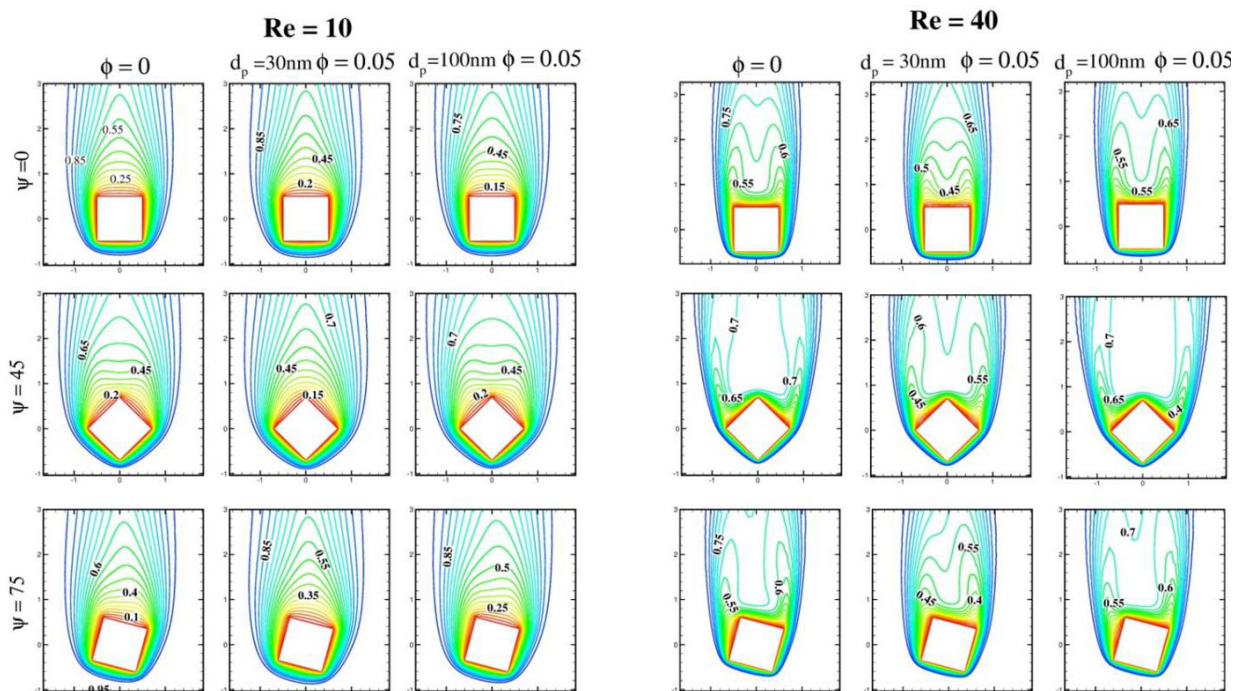


Fig. 2. Variation of isotherm contour with  $Re$ ,  $d_{np}$ ,  $\phi$  and orientation angle ( $\psi$ )

angle of the cylinder and attained the maximum value at  $\psi = 45^\circ$ , after that it is decreasing to  $\psi = 90^\circ$  (not indicated in Fig. 1). Crowding of isotherm contours indicated that reaction that occurs near the cylinder suppresses the isotherms close to the surface of the cylinder thereby resulting in the thin thermal boundary layers. Next, with nanofluids, such as the addition of  $NPs$  in the base fluids, the thermal boundary layers are seen to be much thinner as compared to the pure fluids (water), and as a result, the isotherm contours are much denser near the surface of cylinder irrespective of the values of  $Re$ ,  $\psi$  and  $d_{np}$ . This effect becomes more effective as the value of the Reynolds number progressive increases. Hence, one can expect some enhancement in heat transfer in the presence of nanofluids as compared to pure fluids. Indeed this assertion is borne out by the Nusselt number results presented in the next section.

### 3.3. Effect of orientation of cylinder

Figure 3 represents the orientation effect of square cylinder on average Nusselt Number,  $Nu_{avg}$ , at different volume fractions ( $\phi = 0.1$  and  $\phi = 0.05$ ), sizes of  $NPs$  ( $d_{np} = 30$  nm and  $d_{np} = 100$  nm) and two values of Reynolds number ( $Re = 10$  and  $Re = 40$ ). At the low value of  $Re$  ( $Re = 10$ ), the orientation effect of the cylinder  $Nu_{avg}$  is almost indistinguishable due to the low inertial effect, and consequently, lower heat transfer occurred for all orientations of the cylinder. As the value of  $Re$  increases ( $Re = 40$ ), the orientation effect on the value of  $Nu_{avg}$  is visible due to the higher inertial effect which directly influences the thermal boundary layer irrespective of  $NPs$  size. It can be seen that the thermal boundary layer for the square cylinder at  $45^\circ$  orientation is smaller especially near the upstream and downstream side of the cylinder which is directly related to  $Nu_{avg} \sim 1/\delta_{th}$ . This is also consistent with the isotherm contour shown in Fig. 2. It is seen that the heat transfer from the square cylinder at  $45^\circ$  orientation generated large heat transfer as compared to other orientations of the cylinder.

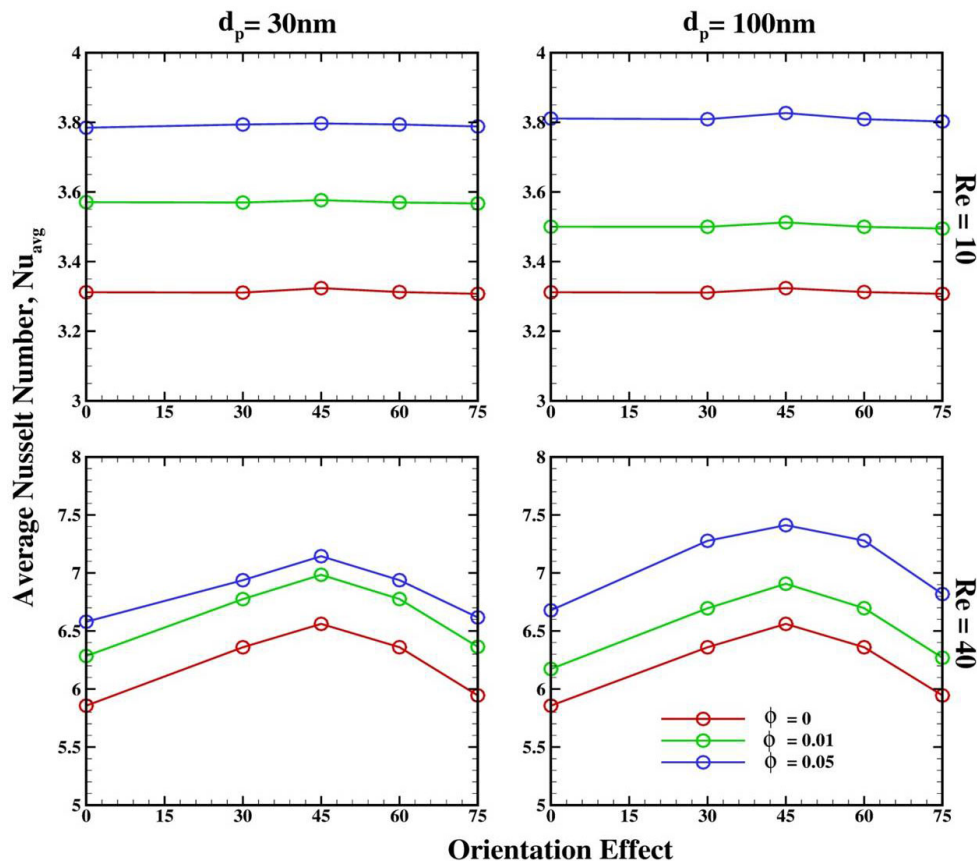


Fig. 3. Variation of average Nusselt number with orientation angle at different values of  $Re$ ,  $\phi$  and  $d_{np}$

Next, the effect of  $\phi$  and  $d_{np}$  can be seen for  $45^\circ$  orientated square cylinders. It is better to represent the variation of heat transfer enhancement ( $E = Nu_{avg}/Nu_{avg,\phi=0}$ ) with  $NPs$  volume fraction,  $\phi$ , is represented at the different sizes of nanoparticles,  $d_{np}$ . From Fig. 4, it is observed that at the small size of  $NPs$  (such as 30 nm, 50 nm), the value of  $E$  increases with  $\phi$  up to the optimum value, after that it starts to deteriorate. As the size of  $NPs$  are large (such as 60 nm and 100 nm), the value of  $E$  gradually increases with  $\phi$  at a fixed value of  $Re$ . This is due to the effective Reynolds number being higher than its global value of Reynolds number in the case of nanofluids containing large  $NPs$  of 60 nm in size, thereby rate heat transfer increases with  $\phi$ .

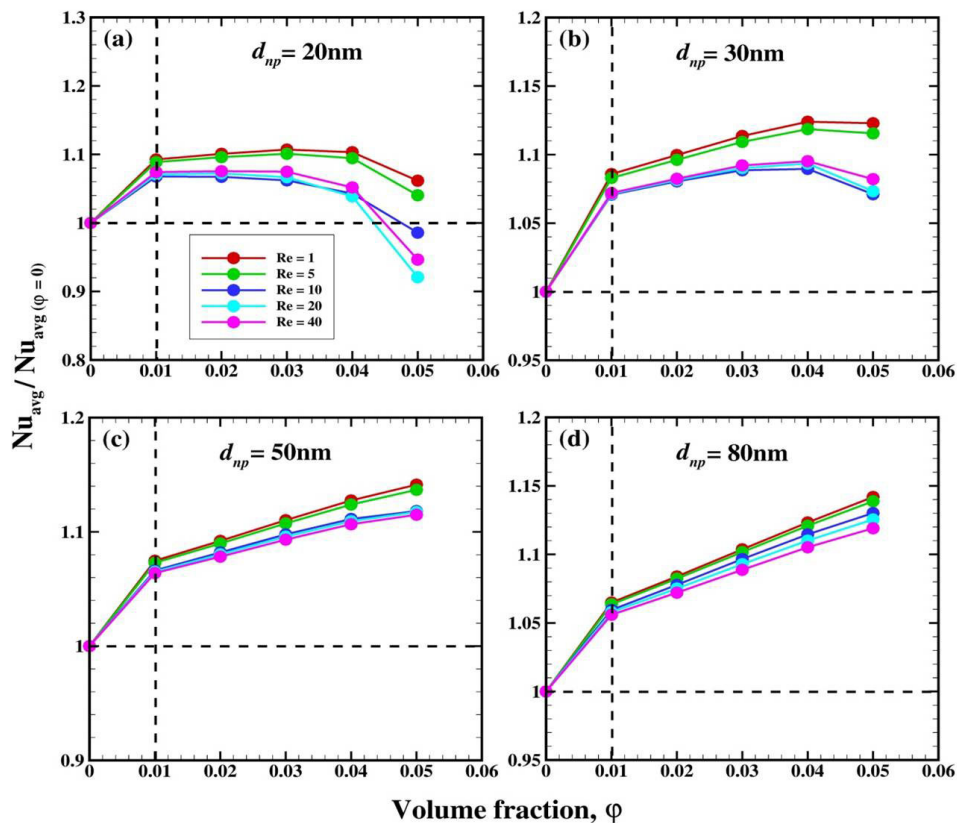


Fig. 4. Variation of  $E$  (for  $45^\circ$  inclined square cylinder) with  $\phi$  of CuO  $NPs$

From the application point of view, the average Nusselt number for  $45^\circ$  orientated square cylinder (optimum orientation of the cylinder) is correlated by using a simple expression for different sizes of  $NPs$  (30 nm to 100 nm) which is used to find out the intermediate values of  $\phi$  and  $Re$  over the ranges of condition  $1 \leq Re \leq 40$  and  $0.00 \leq \phi \leq 0.05$ .

$$Nu_{avg} = \frac{a}{Re} \frac{(1 + bRe^c)}{(1 + e\phi^g)} (1 + d\phi) \quad (5)$$

In Eq. (5), the values of the fitting parameters obtained through the non-linear regression analysis are given in Table 2.

Table 2. The fitting parameter value for the average Nusselt number

$NPs$	$d_{np}$	$a$	$b$	$c$	$d$	$e$	$g$	Avg % error	Max % error
CuO	30 nm	26.981	0.765	0.734	-15.279	-9.2171	0.771	8.53	23.64
	100 nm	20.925	1.056	0.793	-4.7873	-5.7873	0.913	6.87	21.73

#### 4. CONCLUSIONS

A numerical study of laminar, incompressible 2D heat transfers of CuO-water-based nanofluids past a heated square cylinder at different orientations (0–90°) in an infinite domain of nanofluids was conducted. For Reynolds number (1–40), nanoparticle volume fraction (0–0.05), size of the NPs (30–100 nm), the orientation of square cylinder, the following conclusions can be drawn.

- The crowding of isotherm contours near the cylinder increased with the orientation of the square cylinder and attained the maximum crowding at 45° orientated square cylinder which led to the decrease of the thermal boundary layer.
- The average Nusselt number of a square cylinder at low Reynolds number is indistinguishable regardless of the values of  $\phi$  and  $d_{np}$ , whereas, in the case of higher Reynolds number, there is an optimum value of at 45° orientated square cylinder. It starts to deteriorate with the further increasing the orientation angle.
- Finally developed the simple correlation for the average Nusselt number is  $Nu_{avg}$  in the given range of conditions.

#### SYMBOLS

$a$	side length, m
$d_{np}$	diameter of nanoparticles, nm
$D_{\infty}$	diameter of nanoparticles, nm
$h$	heat transfer coefficient, dimensionless
$k_{nf}$	thermal conductivity of nanofluid, $W \cdot m^{-1} \cdot K^{-1}$
$k_{bf}$	thermal conductivity of base fluid, $W \cdot m^{-1} \cdot K^{-1}$
$Nu_{avg}$	average Nusselt number, dimensionless
$N$	total number of elements in the computational domain, dimensionless
$Re$	Reynolds number, dimensionless
$T_{\infty}$	temperature at inlet, K
$T_w$	temperature at wall, K
$V_{\infty}$	velocity at inlet, m/s
$\Psi$	orientation angle of square cylinder, deg
$\rho$	density of fluid, $kg \cdot m^{-3}$
$\mu$	viscosity of fluid, Pa·s
$\rho_{np}$	density of nanoparticle, $kg \cdot m^{-3}$
$\rho_{bf}$	density of base fluid, $kg \cdot m^{-3}$
$\rho_{nf}$	density of nano fluid, $kg \cdot m^{-3}$
$\mu_{nf}$	viscosity of nano fluid, Pa·s
$\mu_{bf}$	viscosity of base fluid, Pa·s
$nf$	nano fluid
$bf$	base fluid

#### REFERENCES

- Chhabra R.P., Richardson J.F., 2011. *Non-Newtonian flow and applied rheology. Engineering applications*. 2nd edition. Butterworth-Heinemann. DOI: [10.1016/B978-0-7506-8532-0.X0001-7](https://doi.org/10.1016/B978-0-7506-8532-0.X0001-7).
- Etmnian-Farooji V., Ebrahimi-Bajestan E., Niazmand H., Wongwises S., 2012. Unconfined laminar nanofluid flow and heat transfer around a square cylinder. *Int. J. Heat Mass Transf.*, 55, 1475–1485. DOI: [10.1016/j.ijheatmasstransfer.2011.10.030](https://doi.org/10.1016/j.ijheatmasstransfer.2011.10.030).

- Kaur J., Melnik R., Tiwari A.K., 2021. Forced convection heat transfer study of a blunt-headed cylinder in non-Newtonian power-law fluids. *Int. J. Chem. Reactor Eng.*, 19, 673–688. DOI: [10.1515/ijcre-2020-0170](https://doi.org/10.1515/ijcre-2020-0170).
- Koo J.C., Kleinstreuer C., 2004. A new thermal conductivity model for nanofluids. *J. Nanopart. Res.*, 6, 577–588. DOI: [10.1007/s11051-004-3170-5](https://doi.org/10.1007/s11051-004-3170-5).
- Masoumi N., Sohrabi N., Behzadmehr A., 2009. A new model for calculating the effective viscosity of nanofluids. *J. Phys. D: Appl. Phys.*, 42, 055501. DOI: [10.1088/0022-3727/42/5/055501](https://doi.org/10.1088/0022-3727/42/5/055501).
- Pak B.C., Cho Y.I., 1998. Hydrodynamic and heat transfer study of dispersed fluid with submicron metallic oxide particles. *Exp. Heat Transfer*, 11, 151–170. DOI: [10.1080/08916159808946559](https://doi.org/10.1080/08916159808946559).
- Valipour M.S., Ghadi A.Z., 2011. Numerical investigation of fluid flow and heat transfer around a solid circular cylinder utilizing nanofluid. *Int. Commun. Heat Mass Transfer*, 38, 1296–1304. DOI: [10.1016/j.icheatmasstransfer.2011.06.007](https://doi.org/10.1016/j.icheatmasstransfer.2011.06.007).
- Xuan Y.W., Roetzel W., 2000. Conceptions for heat transfer correlation of nanofluids. *Int. J. Heat Mass Transfer*, 43, 3701–3707. DOI: [10.1016/S0017-9310\(99\)00369-5](https://doi.org/10.1016/S0017-9310(99)00369-5).

*Received 16 February 2022*

*Received in revised form 22 March 2022*

*Accepted 6 April 2022*